Applied Catalysis B: Environmental 99 (2010) 103–110

Contents lists available at ScienceDirect

Applied Catalysis B: Environmental

journal homepage: www.elsevier.com/locate/apcatb

Total oxidation of CO at ambient temperature using copper manganese oxide catalysts prepared by a redox method

Eric C. Njagi[a], Chun-Hu Chen[a], Homer Genuino[a], Hugo Galindo[a], Hui Huang[a], Steven L. Suib[a,b,*]

[a] Department of Chemistry, University of Connecticut, Storrs, CT 06269-3060, USA
[b] Department of Chemical Engineering, and Institute of Materials Science, University of Connecticut, U-3060, 55 North Eagleville Rd., Storrs, CT 06269-3060, USA

ARTICLE INFO

Article history:
Received 23 November 2009
Received in revised form 1 June 2010
Accepted 7 June 2010
Available online 11 June 2010

Keywords:
Amorphous manganese oxide
Copper manganese oxides
Hopcalite
Ambient temperature CO oxidation
Water poisoning

ABSTRACT

Binary copper manganese oxides were prepared by a novel redox method and their catalytic activity for CO oxidation at ambient temperature evaluated. The catalytic activity was found to be high, and compared favorably with a commercial Hopcalite catalyst. The most active catalyst was able to completely oxidize CO at ambient temperature. Catalytic activity decay, most likely due to carbon dioxide retention was observed. The catalysts were deactivated by moisture but expelling water at moderate temperatures easily restored their catalytic activity. The catalysts were characterized by means of BET, FE-SEM, TEM, EDAX, XPS, TPD and X-ray powder diffraction. The optimum copper loading was determined to be ~9% of the manganese content.

1. Introduction

The development of low temperature carbon monoxide oxidation catalysts has become an important research topic due to the many potential areas of application in industrial, environmental and domestic fields. These include chemical sensors [1], CO_2 lasers [2], proton exchange membrane fuel cells [3–5], automobile emissions [6] and air purification devices [7]. Catalysts made of nanoparticles of noble metals (e.g. Pt, Ru, and Au) supported on reducible metal oxides have high catalytic activity for CO oxidation [1,8–11]. Gold nanoparticles deposited on reducible semiconductor metal oxides, hydroxides of alkaline earth metals, and amorphous ZrO_2 are highly active for CO oxidation at ambient and sub-ambient temperatures and unlike transition metal oxides they are not susceptible to moisture poisoning [2,4,12–16]. However, the scarcity and high cost of precious metals have long motivated the search for substitute catalysts [17]. Considerable efforts have been directed towards the design of CO oxidation catalysts based on transition metal oxides or composite transition metal oxides [5,9,17,18]. Among the transition metal oxides, tricobalt tetraoxide (Co_3O_4) is the most active for low temperature CO oxidation, but Co_3O_4 is severely deactivated even by trace amounts of moisture found in normal feed gas [19,20]. Recently Xiaowei and coworkers have synthesized Co_3O_4 nanorods, which completely oxidized CO in a normal feed gas below 0 °C [21].

Hopcalite (copper manganese oxide) is the most widely used commercial catalyst for respiratory protection because of its low cost [22]. Hopcalite is used extensively in air purification devices for respiratory protection in mining, the military, and in industrial emission control [23,24]. Unfortunately, current commercial Hopcalite catalysts have low activity at ambient temperature and are also rapidly deactivated by moisture [23–25]. Development of cost effective catalysts with high catalytic activity for CO oxidation at ambient temperature for prolonged periods in diverse oxidation environments remains a challenge. The structural, morphological and catalytic properties of copper manganese oxide catalysts are greatly influenced by preparation methods [26–29]. Conventionally, copper manganese oxide catalysts are prepared using the co-precipitation method from mixed metal nitrates and sodium carbonate [27] or the sol–gel method [22]. Recently, Tang et al. have synthesized nanocrystalline copper manganese oxide catalysts using the supercritical antisolvent precipitation method and found them to be more than twice as active as the conventionally prepared Hopcalite catalysts for the oxidation of CO [30]. They attributed the high catalytic activity to the nanocrystalline and homogeneous nature of the synthesized copper manganese oxides.

In this study, copper manganese oxides were prepared using a novel redox method and their catalytic performance for CO oxidation at ambient temperature under different conditions studied. This novel redox method allowed for room temperature synthesis

* Corresponding author at: Department of Chemical Engineering, and Institute of Materials Science, University of Connecticut, U-3060, 55 North Eagleville Rd., Storrs, CT 06269-3060, USA. Tel.: +1 8604862797.
E-mail address: steven.suib@uconn.edu (S.L. Suib).

0926-3373/$ – see front matter © 2010 Elsevier B.V. All rights reserved.
doi:10.1016/j.apcatb.2010.06.006

of amorphous copper manganese oxides with high surface areas, and high catalytic activity for CO oxidation at ambient temperature. In addition, these catalysts showed enhanced resistance to water poisoning. The structural, morphological, and catalytic properties of catalysts prepared using the redox method are compared to those of a commercial Hopcalite catalyst.

2. Experimental

2.1. Preparation of catalysts

All the chemicals used in this study were of analytical grade, and were used without further purification. Amorphous manganese oxide (AMO) catalyst was prepared by the reduction of potassium permanganate ($KMnO_4$, Fisher Scientific) with manganese (II) acetate tetrahydrate ($Mn(CH_3COO)_2{\cdot}4H_2O$, Alfa Aesar). A solution of $Mn(CH_3COO)_2{\cdot}4H_2O$ (22.05 g in 50 mL H_2O) was added dropwise to a solution of $KMnO_4$ (9.48 g in 50 mL H_2O) under vigorous stirring. The resultant precipitate was stirred continuously for 24 h, filtered, washed, vacuum dried, and ground into powder. The above procedure was modified to prepare binary copper manganese oxides by adding 4.61 g of copper (II) nitrate ($Cu(NO_3)_2{\cdot}2.5H_2O$, Mallinckrodt Baker) to the manganese (II) acetate solution before reduction. A copper manganese oxide precursor (CuMnOx-A) was obtained after vacuum drying the precipitate. The precursor was calcined in air for 2 h at 300 °C and the resultant sample designated CuMnOx-B. The amount of copper added was varied to synthesize catalysts with nominal copper/manganese molar ratios of 5/95, 10/90, 15/85, 20/80, 30/70, 40/60, and 50/50. A commercial Hopcalite catalyst (Carulite 300 granular catalyst) was purchased from Carus Chemical Company and used as a reference. The granules were crushed into powder and used without any further pretreatment.

2.2. Characterization of catalysts

2.2.1. X-ray powder diffraction

X-ray powder diffraction patterns of the samples were obtained using a Scintag 2000 PDS diffractometer. The wavelength of Cu-Kα X-ray radiation used was 1.5418 Å while the beam voltage and current were 45 kV and 40 mA, respectively.

2.2.2. Electron microscopy

The morphology of the samples was studied using field emission scanning electron microscopy (FE-SEM) and transmission electron microscopy (TEM). The FE-SEM micrographs were taken using a Zeiss DSM 982 Gemini microscope equipped with a Schottky emitter at an accelerating voltage of 10–20 kV and a beam current of 1 μA. Samples were prepared for analyses by dispersing them in ethanol and coating a monolayer on a gold-coated silicon wafer. TEM images were obtained with a FEI Tecnai T12 TEM at an accelerating voltage of 200 kV. Powder samples were dispersed ultrasonically in 2-propanol, and the suspension was deposited on a Quantafoil holey carbon-coated copper grid.

2.2.3. BET analysis

The specific surface areas of the samples were determined using the Brunauer–Emmett–Teller (BET) method by performing nitrogen sorption measurements using a Micrometrics ASAP 2010 instrument. The adsorption and desorption experiments were done at 77 K after initial pretreatment of the samples by degassing at 120 °C for 2 h.

2.2.4. Energy dispersive X-ray (EDAX) analysis

The chemical composition of the samples was determined using a scanning electron microscope (SEM) equipped with an AMRAY/LICO Model 9800 energy dispersive X-ray (EDAX) analyzer at 20.0 kV and an acquisition lifetime of 100 s. An average of values measured at three random locations was used to determine the concentration of chemical components. The standardless ZAF method was used to quantify the elements present in the samples with an accuracy of ±2%.

2.2.5. Temperature programmed desorption (TPD)

Temperature programmed desorption (TPD) was used to identify gases adsorbed on the surface of the catalysts after CO oxidation tests. The catalyst (100 mg) was packed into a quartz tube and loaded into a tubular furnace controlled by an Omega temperature controller. The sample was pretreated by flowing UHP He (30 sccm) for 2 h at 180 °C then cooled naturally to room temperature. Subsequently, the feed gas (1% CO, 20% O_2, 5% N_2 in He) was introduced at a flow rate of 30 sccm and the reaction allowed to proceed for 14 h. The sample was then purged with UHP He (30 sccm) for about 1 h to remove any surface physisorbed gases and residual feed gas from the streams. After purging, the sample was heated under a flow of He (30 sccm) from room temperature to 500 °C at a ramp rate of 10 °C/min. The desorbed gases were monitored using a MKS-UTI PPT quadrupole mass spectrometer.

2.2.6. X-ray photoelectron spectroscopy (XPS) analysis

The binding energies of elements in the samples were determined using a PerkinElmer Physical Electronics 5300 X-ray photoelectron spectrometer equipped with a hemispherical analyzer. Al Kα radiation was used at 250 W X-ray power and a pass energy of 50 eV. The base pressure of the system was 5.0×10^{-9} Torr. The signal from adventitious carbon (assumed to have a binding energy of 284.6 eV) was used as a reference for binding energies.

2.2.7. Catalytic activity tests

The catalytic tests were performed in a quartz tubular fixed bed flow reactor at atmospheric pressure with 100 mg of the catalyst. All the gases used in this study were purchased from Airgas East Inc. (Salem, NH), and were of ultra high purity (UHP). The catalysts were pretreated in flowing He (50 mL/min) at 180 °C for 2 h to completely dry and remove any adsorbed species on the surface. The gaseous reactants were premixed in a tank and typically consisted of 1% CO, 2% O_2 and 5% N_2 in He. Application relevant (i.e. air purification systems) tests were performed using 1% CO, 20% O_2, 5% N_2 in He. Nitrogen was included in the feed as an internal standard. The space velocity was varied between 12,000–35,000 mL h^{-1} $g_{cat}{}^{-1}$ using mass flow controllers. The feed and product gas streams were analyzed by a SRI 8610C gas chromatograph (GC) equipped with a 6′ molecular sieve, a 6′ silica gel column, and a thermal conductivity detector (TCD). Catalytic tests with moist feed gas (~3% H_2O) were done analogously by passing the feed gas through a water bubbler at room temperature.

3. Results

3.1. Preparation of catalysts

The amount (mol% of the manganese content) of copper incorporated into various samples synthesized using the redox method was determined using EDAX and is shown in Fig. 1. These results indicate it is not possible to incorporate all copper into the catalysts beyond 5% loading presumably because Cu^{2+} ions are not directly involved in the redox reaction but are trapped in the resultant amorphous manganese oxide framework.

The excess Cu^{2+} ions remain in solution and are together with any weakly bound Cu^{2+} ions removed from the retentate during the filtering and washing steps. This is evident from the bluish color

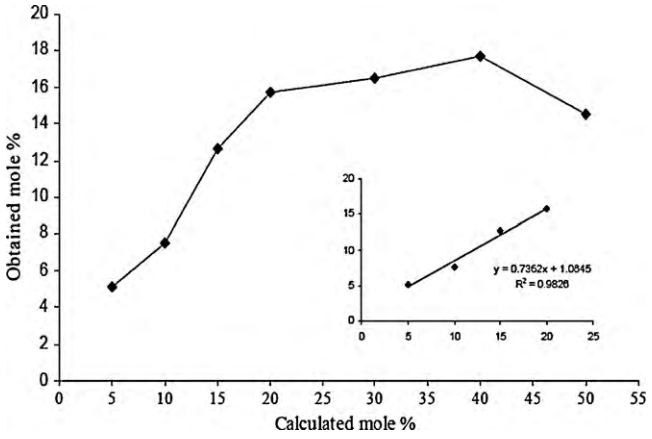

Fig. 1. Calculated and obtained amount of copper (mol%) in samples prepared using the redox method.

of the filtrates. However, it is possible to obtain reproducible copper loadings using the redox method. There is a linear relationship (inset graph) between calculated (up to 20%) and obtained amounts of copper in the samples implying it is possible to obtain exact copper loading in this range, using excess amounts of copper where necessary.

3.2. Powder XRD analysis

The powder XRD patterns of the reference Hopcalite catalyst and samples prepared using the redox method are shown in Fig. 2. The reference Hopcalite catalyst, AMO, and copper manganese oxide samples (CuMnOx-A and CuMnOx-B) prepared using the redox method do not have distinct diffraction peaks implying they are amorphous.

The amorphous nature of these catalysts was confirmed using small area electron diffraction (SAED) analysis (*vide infra*).

3.3. Morphology of the catalysts

The morphology of the samples was studied by field emission scanning electron microscopy (FE-SEM) and transmission electron microscopy.

Fig. 3(a) shows the FE-SEM image of AMO. The sample is composed of aggregates of nanoparticles. Closer observations of the AMO sample using TEM (Fig. 3(b)) reveals that the aggregates are composed of fine nanoparticles with a diameter range around

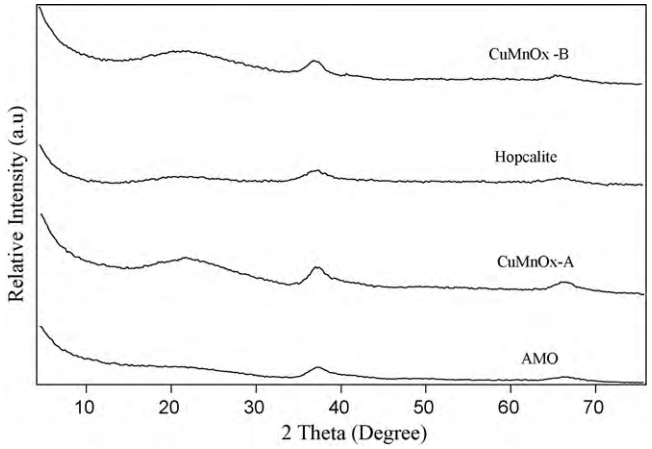

Fig. 2. Powder XRD patterns of various manganese oxide catalysts.

Table 1
Surface areas of various manganese catalysts.

Sample	Hopcalite	AMO	CuMnOx-A	CuMnOx-B
Surface area (m^2/g)	308	312	376	297

10–15 nm. Commercial Hopcalite, AMO, and copper manganese oxide samples prepared using the redox method have similar morphologies as shown in Fig. 3(b–d). Selected area electron diffraction (SAED) patterns (insets) reveal these materials are amorphous due to lack of diffraction rings or spot patterns, in agreement with powder XRD results.

3.4. Surface area of the catalysts

The BET surface areas (Table 1) of Hopcalite, AMO and the calcined copper manganese oxide (CuMnOx-B) sample were comparable and in the range of 297–312 $m^2\ g^{-1}$. Calcining the copper manganese precursor (CuMnOx-A) led to a significant decrease in the surface area of the resultant sample (CuMnOx-B).

3.5. Composition of the catalysts

The elemental composition of various manganese oxide catalysts is shown in Table 2. Standardless elemental analysis of Hopcalite catalyst by EDAX gave a copper/manganese atomic ratio of 29/67 with small amounts of potassium and calcium. AMO had the highest amount of manganese and potassium while copper manganese oxides (CuMnOx-A and CuMnOx-B) prepared by the redox method had comparable but lower copper content than the reference Hopcalite catalyst.

These EDAX results (average of values measured at three random locations) and the morphological uniformity of the samples (examined by FE-SEM and TEM) suggest that the elemental composition of these samples is homogeneous. Commercial Hopcalite is usually sold in granular form and contains small amounts of calcium [22]. Calcium is most likely a constituent of the binder used to make Hopcalite granules [31,32].

3.6. TPD analysis

Temperature programmed desorption (TPD) using the reaction gas mixture was performed to investigate possible causes of activity decay with time. As shown in Fig. 4, carbon dioxide desorbs from the catalyst surface suggesting CO_2 retention is one of the processes responsible for activity decay of catalysts at low temperatures.

In addition, a significant amount of water desorbs from the catalyst surface at about 180 °C implying an increase in surface moisture content could also contribute to activity decay.

3.7. XPS studies

Fig. 5 shows the Mn 2p spectra of Hopcalite and samples prepared using the redox method. The Mn $2p_{3/2}$ binding energies for Hopcalite, AMO, CuMnOx-A and CuMnOx-B were 643.7, 643.4, 643.7, and 642.3 eV, respectively. All these values are higher than

Table 2
Composition of various manganese oxide catalysts.

Sample	Composition (at.%)			
	Mn	Cu	K	Ca
Hopcalite	66.6	29.0	2.9	1.7
AMO	89.0	0	11.0	0
CuMnOx-A	86.1	9.1	4.7	0
CuMnOx-B	86.7	8.9	4.4	0

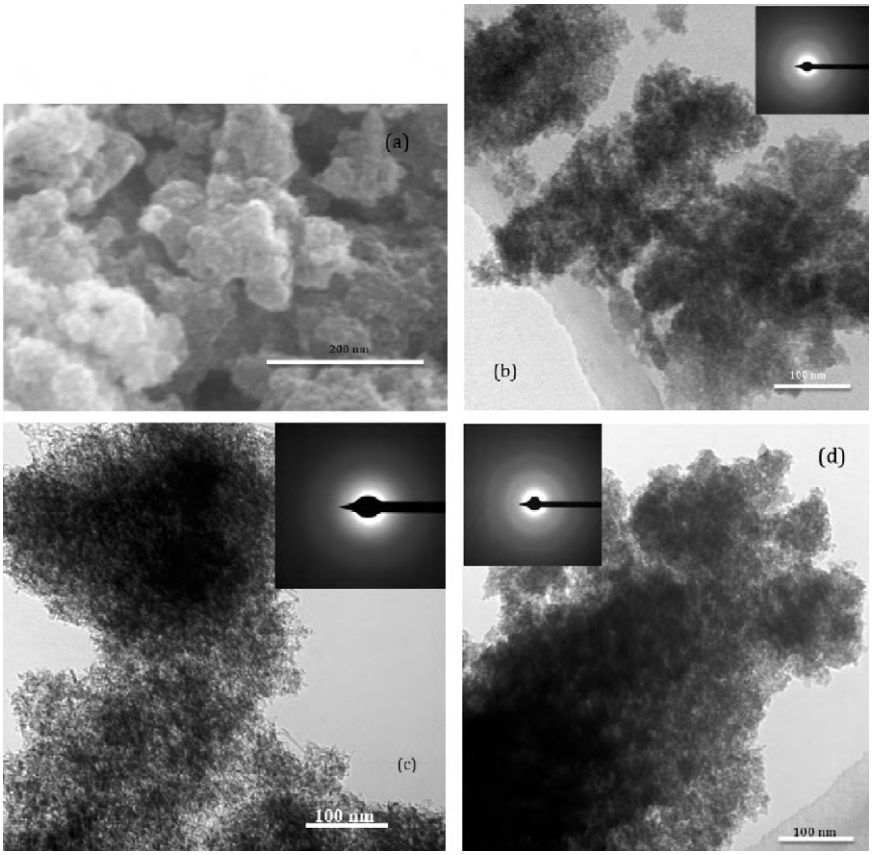

Fig. 3. FE-SEM image of: (a) AMO and TEM images of: (b) AMO, (c) CuMnOx-B, and (d) Hopcalite.

the Mn $2p_{3/2}$ binding energy of Mn^{4+} (642.2 eV) in MnO_2 reported in the literature [33]. The full width at half maximum (FWHM) values (see Table 3) suggests one of the possible reasons for these high values is line broadening resulting from multiplet splitting [34]. The small differences in the binding energies of Mn^{2+}, Mn^{3+}, and Mn^{4+} compounded by the aforementioned lines broadening made it very difficult to precisely determine the oxidation state(s) of Mn in the samples. We determined the average oxidation state (AOS) of manganese in AMO to be 3.8 using a potentiometric titration method described in the literature [35,36]. Though not conclusive, the high binding energy values of Mn $2p_{3/2}$ and our redox titration results for the AMO sample suggest a mixed valent environment with Mn^{4+} being predominant. More detailed investigations using a higher resolution XPS are currently in progress to determine the chemical state of manganese.

The Mn $2p_{3/2}$ binding energy of CuMnOx-B is shifted to the lower energy side relative to the other samples suggesting it has a higher amount of lower valence manganese ions. Interestingly, CuMnOx-B is the most active catalyst among those tested in this study (*vide infra*).

Fig. 6 shows the O 1s spectra of Hopcalite and samples prepared using the redox method. The O 1s binding energies of Hopcalite, AMO, CuMnOx-A, and CuMnOx-B are 530.0, 530.3, 530.4, and 529.5 eV, respectively. These binding energies suggest that the

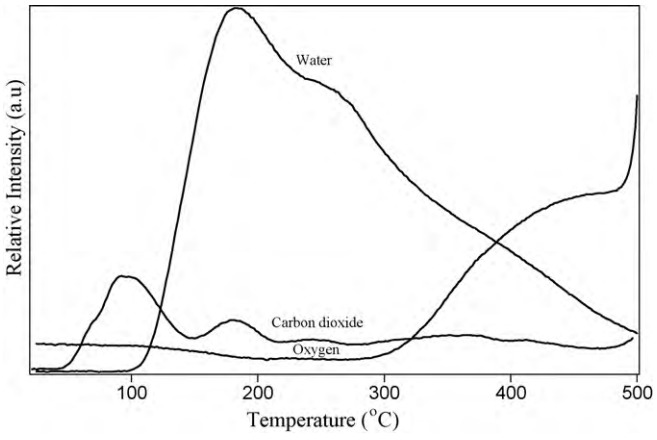

Fig. 4. A representative temperature programmed desorption profile of CuMnOx-A sample.

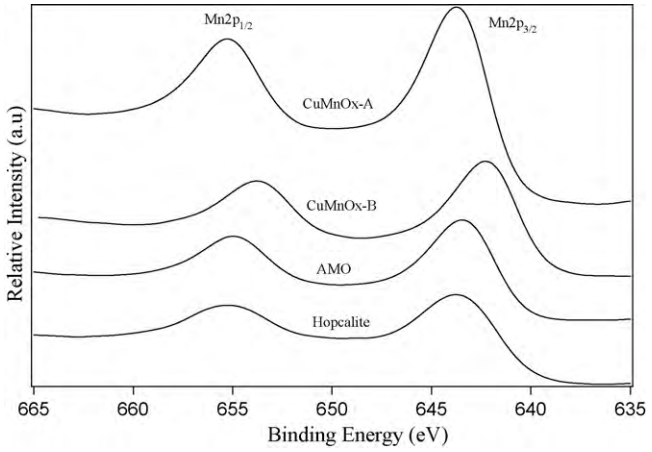

Fig. 5. Mn 2p XPS spectra of Hopcalite and samples prepared using the redox method.

Table 3
Binding energies of Mn 2p and the corresponding full width at half maximum (FWHM) values.

Sample	Binding energies (eV)			
	Mn_{2p}		FWHM[a]	
	$2p_{3/2}$	$2p_{1/2}$	$2p_{3/2}$	$2p_{1/2}$
Hopcalite	643.7	654.6	4.9	5.4
AMO	643.4	654.8	3.4	3.3
CuMnOx-A	643.7	655.1	3.2	3.2
CuMnOx-B	642.3	653.7	3.4	3.3

[a] Full width at half maximum.

oxide (O^{2-}) species are predominantly near the surface of the samples [33,34]. Noticeably, the O 1s binding energy of CuMnOx-B sample is shifted lower relative to the other three samples suggesting a favorable influence on the mobility of lattice oxygen.

It is generally accepted copper exist in the (II) oxidation state in binary copper manganese oxides [22,28,37]. Fig. 7 shows Cu 2p XPS spectra of Hopcalite and CuMnOx-A samples. The binding energies of Cu $2p_{3/2}$ for Hopcalite and CuMnOx-A are 935.6 and 935.8 eV, respectively. Shake-up peaks (characteristic of Cu^{2+}) are also present in the spectra. These results indicate that at least some of the Cu^{2+} phase is predominantly in the near surface of the catalysts.

3.8. Catalytic activity

3.8.1. Catalytic performance at different temperatures

The catalytic performance of the catalysts for CO oxidation after 1 h on-stream at each temperature is shown in Fig. 8. A fresh catalyst was used to test catalytic activity at each temperature. The catalyst synthesized using the redox method and calcined in air for 2 h at 300 °C (CuMnOx-B) totally oxidized CO at ambient and all subsequent temperatures. The precursor catalyst (CuMnOx-A) was less active than CuMnOx-B at low temperatures and only oxidized CO completely at 70 °C. On the other hand, the catalytic performance of AMO and the reference Hopcalite catalyst at low temperatures was less than that of CuMnOx-A. AMO did not have any observable catalytic activity at 30 °C after 1 h.

The catalytic activity of copper manganese oxides is highly dependent on the method of synthesis. Depending on the preparation method, several authors have observed catalytic activity maxima for copper manganese oxide catalysts at a copper/manganese atomic ratio of 10/90, 20/80, and 50/50 [22,26,38]. We decided to initially load our catalysts with about 10% copper and found them to be highly active for CO oxidation. To investigate

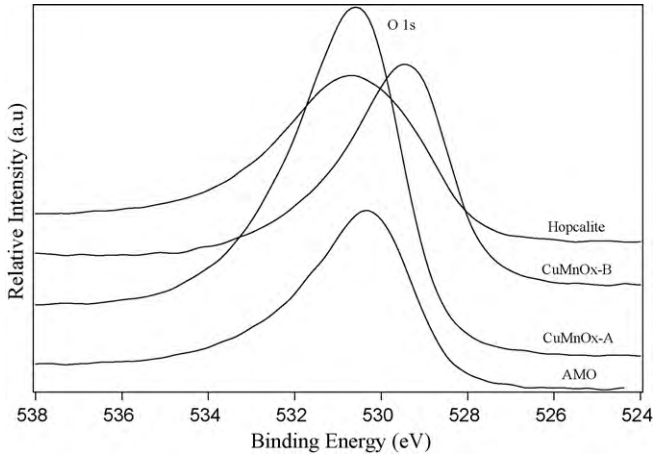

Fig. 6. O 1s XPS spectra of Hopcalite and samples prepared using the redox method.

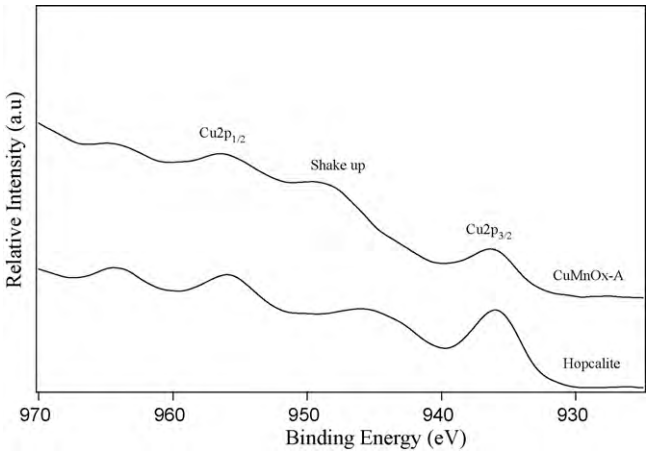

Fig. 7. Cu 2p XPS spectra of Hopcalite and CuMnOx-A samples.

the effect of copper loading on the catalytic activity of copper manganese oxides synthesized using the redox method, samples with 5, 8.9 (CuMnOx-B), and 14.9% copper content were tested at 25 °C. The CO conversion after 1 h on-stream at 25 °C was 21, 100, and 43%, respectively. This suggests a catalytic maximum at a copper loading of ~9% for samples prepared using the redox method.

3.8.2. Effect of space velocity

The effect of space velocity on catalytic activity after 1 h on-stream at each temperature was investigated using AMO. As shown in Fig. 9, higher conversions were observed at lower space velocities. AMO completely oxidized CO at 40 °C both at space velocities of 12,000 and 17,500 mL h^{-1} $g_{cat}{}^{-1}$.

3.8.3. Effect of oxygen concentration in the feed gas

To study the effect of oxygen concentration on catalytic activity and mimic application relevant conditions (i.e. respiratory protection), experiments were performed using a feed gas consisting of 1% CO, 20% O_2 and 5% N_2 in helium. AMO showed significantly higher catalytic activity at low temperatures when the oxygen concentration was increased from 2% to 20% as shown in Fig. 10. Catalytic conversion of CO at ambient temperature increased from 0% to over 20%.

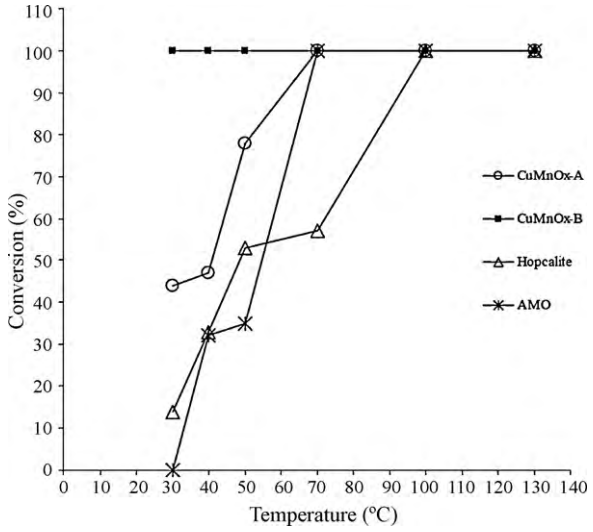

Fig. 8. Effect of temperature on the catalytic performance of various catalysts. Catalyst: 100 mg, space velocity: 35,000 mL h^{-1} $g_{cat}{}^{-1}$, feed gas: 1% CO, 2% O_2, and 5% N_2 in helium.

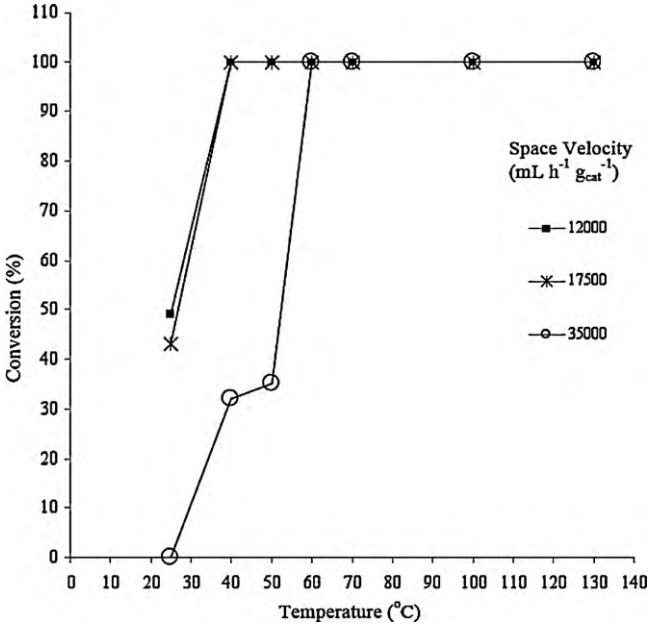

Fig. 9. Effect of space velocity on the catalytic activity of AMO. Catalyst: 100 mg, feed gas: 1% CO, 2% O_2, and 5% N_2 in helium.

AMO completely converted CO to CO_2 at 50 °C when the concentration of oxygen in the feed was increased to 20%.

3.8.4. Stability studies

The catalytic activity of copper manganese oxides prepared using the redox method was measured at 25 °C for 24 h to determine their lifetimes. As shown in Fig. 11, CO conversion decreased gradually for both the precursor (CuMnOx-A) and the calcined (CuMnOx-B) catalysts.

However, the calcined catalyst (CuMnOx-B) was significantly more stable than the precursor catalyst (CuMnOx-A) and showed over 50% CO conversion after 24 h.

The stability of AMO and Hopcalite catalysts was investigated at 70 °C due to their low catalytic performance at ambient temperature. As shown in Fig. 12, the catalytic activities of both catalysts decay steadily to about 50% after 24 h.

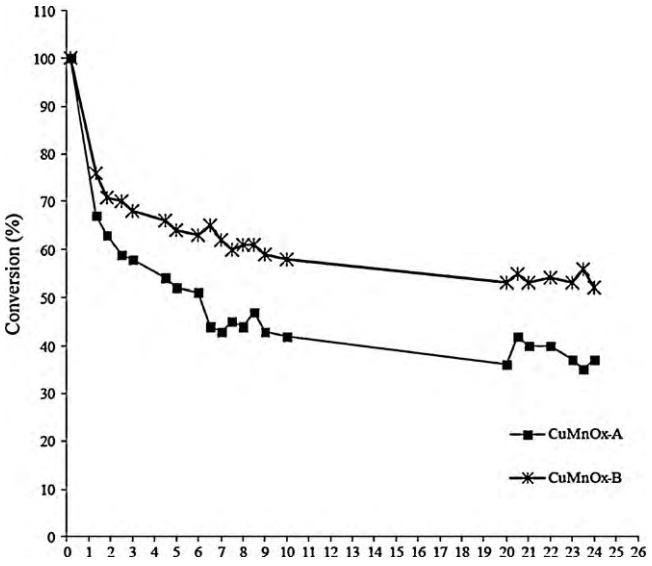

Fig. 11. Catalytic activity of CuMnOx-A and CuMnOx-B catalysts as a function of time at 25 °C. Catalyst: 100 mg, space velocity: 35,000 mL h^{-1} g_{cat}^{-1}, feed gas: 1% CO, 20% O_2, and 5% N_2 in helium.

3.8.5. Effect of moisture

Stability of CO oxidation catalysts under moist air is essential for respiratory applications. The catalytic performance of catalysts synthesized using the redox method under moist conditions was tested at ambient temperature. As shown in Fig. 13, catalytic activities of CuMnOx-A and CuMnOx-B were adversely affected by moisture (~3% water).

Notably, these two catalysts were able to resist water poisoning for 10 min whereas commercial Hopcalite is known to deactivate rapidly under moisture [22]. In addition, the catalytic activities (at 25 °C) of water-poisoned CuMnOx-A and CuMnOx-B samples were fully restored (see Figure S1 in the Supporting Information) by treating them in a stream of helium at 180 °C for 2 h.

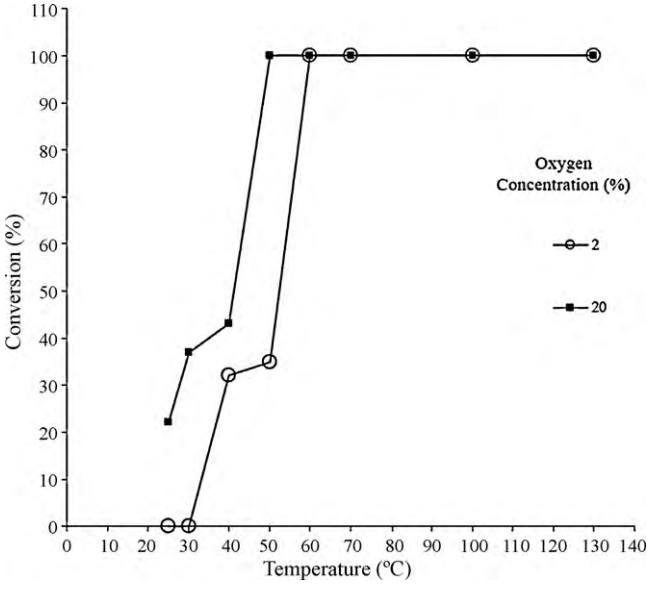

Fig. 10. Effect of oxygen concentration on the catalytic activity of AMO. Catalyst: 100 mg, space velocity: 35,000 mL h^{-1} g_{cat}^{-1}, feed gas: 1% CO, 20% O_2 and 5% N_2 in helium.

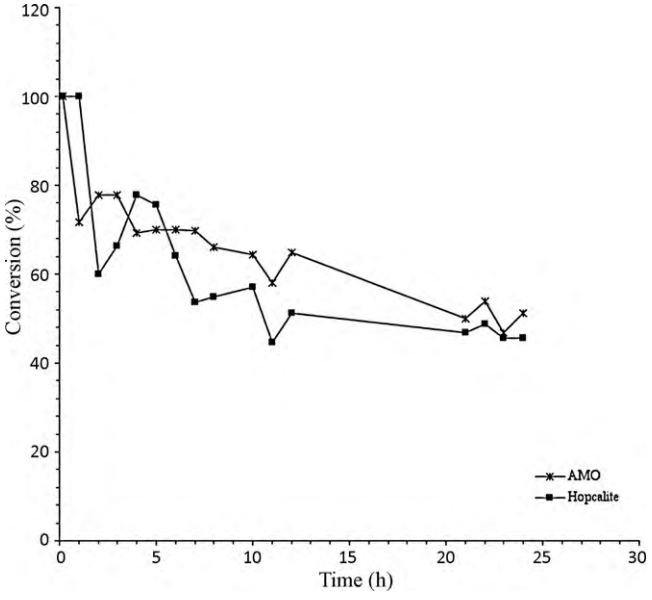

Fig. 12. Catalytic activity of AMO and Hopcalite as a function of time at 70 °C. Catalyst: 100 mg, space velocity: 35,000 mL h^{-1} g_{cat}^{-1}, feed gas: 1% CO, 2% O_2, and 5% N_2 in helium.

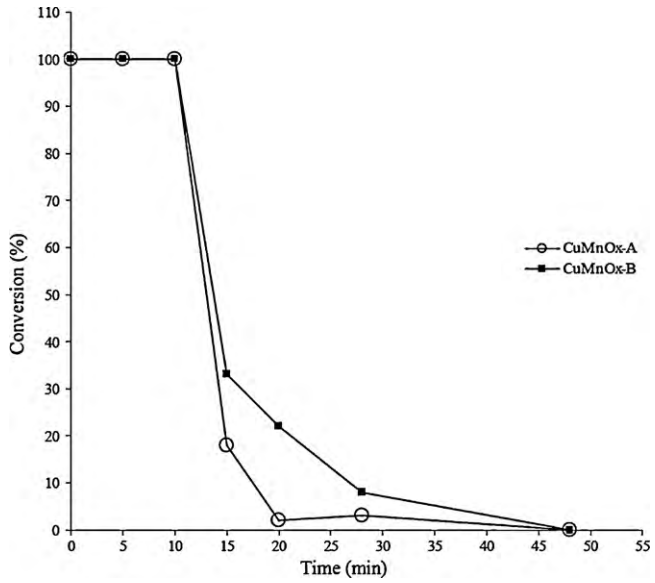

Fig. 13. Effect of moisture on the catalytic activity of CuMnOx-A and CuMnOx-B catalysts at 25 °C. Catalyst: 100 mg, space velocity: 35,000 mL h^{-1} g_{cat}^{-1}, feed gas: 1% CO, 20% O_2, and 5% N_2 in helium.

3.9. Discussion

The catalytic activity of copper manganese oxides for CO oxidation is influenced by a combination of factors including preparation method, surface area, crystallinity, and the presence of Cu^{2+} and Mn^{3+} near the surface [22,26,29]. Hopcalite and catalysts prepared using the redox method were all found to be amorphous and had comparable surface areas. Therefore, the differences in catalytic performance of these catalysts cannot be solely attributed to surface area effects.

Tang et al. have recently prepared copper manganese oxide catalysts using the supercritical antisolvent precipitation method and found them to have significantly higher catalytic activity for CO oxidation compared to conventionally prepared Hopcalite [30]. They attributed the enhancement in catalytic activity to the nanocrystalline and homogeneous nature of the synthesized catalysts, which brings the active components together in the same phase. Similarly, the high precision of our EDAX measurements and the morphological uniformity of the samples (examined by FE-SEM and TEM) suggest that the elemental composition of copper manganese oxides synthesized using the redox method is homogeneous. The nanostructured and homogeneous nature of copper manganese oxides synthesized using the redox method could be among the major factors contributing to their high catalytic activity.

Preliminary XPS results suggest the relative amount of Mn^{2+}, Mn^{3+}, and Mn^{4+} in these catalysts could also be essential for catalytic performance. These XPS results suggest the most active catalyst (CuMnOx-B) had a relatively higher amount of lower valence manganese and loosely bound lattice oxygen. We are now carrying out detailed studies using a higher resolution XPS to resolve the three Mn oxidation states in the near surface of these catalysts.

The catalytic activity of copper manganese oxides is highly dependent on synthesis methods. We observed activity maxima for copper manganese oxide catalysts prepared using the redox at a copper/manganese atomic ratio of ~9/91. Other studies have observed activity maxima at a copper/manganese atomic ratio of ~10/90, ~20/80, and ~50/50 [22,26,38].

The low catalytic performance of Hopcalite and AMO at near ambient temperatures is caused by CO adsorption [39,40]. A clean surface exposed to a mixture of CO and O_2 quickly becomes covered with CO since CO requires a single vacant adsorption site while O_2 requires two adjacent sites. This prevents O_2 adsorption leading to the observed low catalytic activity, except at low CO to O_2 ratios. Consequently, higher catalytic activity at ambient temperature is observed when the concentration of oxygen in the feed gas is increased or the space velocity decreased. The catalytic reaction is also faster at elevated temperatures because CO desorption becomes significant allowing for dissociative O_2 adsorption.

Our TPD results suggest carbon dioxide retention is the main cause of catalytic decay. Hoflund et al. observed a correlation between the rate of decay due to CO_2 retention and the magnitude of catalytic activity increase after outgassing for Au/MnOx catalysts [2]. Au/MnOx catalysts with larger decay rates outgassed more CO_2 and exhibited larger increases in catalytic activity. The catalytic activity was easily restored by pretreatment to remove adsorbed carbon dioxide [2].

The presence of water in the feed gas had a marked poisoning effect on the catalytic activity of CuMnOx-A and CuMnOx-B catalysts. Water is believed to poison the catalyst by adsorbing on oxygen active sites [28]. However, these two catalysts were able to resist water poisoning for 10 min whereas commercial Hopcalite is known to deactivate rapidly under moisture [22]. The catalytic activity was fully restored by expelling moisture at moderate temperature.

4. Conclusion

Copper manganese oxides have been successfully synthesized using a novel redox method and their catalytic activity for CO oxidation at ambient temperature evaluated. The redox method allowed for the synthesis of amorphous catalysts with high surface areas and high catalytic performance. The catalytic performance of catalysts prepared using the redox method compare favorably with a commercial Hopcalite catalyst. The most active copper manganese catalyst (CuMnOx-B) showed a 100% conversion at ambient temperature. The synthesized catalysts have potential applications in respiratory protection systems. Optimization of these catalysts by compositional variation or doping is being explored.

Acknowledgements

The authors are grateful to Dr. F.S. Galasso and Dr. Raymond Joesten for helpful suggestions and discussions, Lei Jin and Anais Espinal for assisting with the catalytic setup. We are grateful to the US Department of Energy, Office of Basic Energy Sciences, Division of Chemical Sciences, Geosciences, and Biological Sciences, for supporting this research.

Appendix A. Supplementary data

Supplementary data associated with this article can be found, in the online version, at doi:10.1016/j.apcatb.2010.06.006.

References

[1] S.D. Gardner, G.B. Hoflund, D.R. Schryer, B.T. Upchurch, E.J. Kielin, Langmuir 7 (1991) 2135.
[2] G.B. Hoflund, S.D. Gardner, D.R. Schryer, B.T. Upchurch, E.J. Kielin, Appl. Catal. B: Environ. 6 (1995) 117.
[3] M. Götz, H. Wendt, Electrochim. Acta 43 (1998) 3637.
[4] A. Luengnaruemitchai, D.T.K. Thoa, S. Osuwan, E. Gulari, Int. J. Hydrogen Energy 30 (2005) 981.
[5] Y. Teng, H. Sakurai, A. Ueda, T. Kobayashi, Int. J. Hydrogen Energy 24 (1999) 355.

[6] Y. Hasegawa, K. Fukumoto, T. Ishima, H. Yamamoto, M. Sano, T. Miyake, Appl. Catal. B: Environ. 89 (2009) 420.
[7] S.H. Taylor, C. Rhodes, Catal. Lett. 101 (2005) 31.
[8] Y.J. Mergler, A. van Aalst, J. van Delft, B.E. Nieuwenhuys, Appl. Catal. B: Environ. 10 (1996) 245.
[9] P. Thormählen, M. Skoglundh, E. Fridell, B. Andersson, J. Catal. 188 (1999) 300.
[10] D.L. Trimm, Z.I. Önsan, Catal. Rev. Sci. Eng. 43 (2001) 31.
[11] Z. Zou, M. Meng, Q. Li, Y. Zha, Mater. Chem. Phys. 109 (2008) 373.
[12] M. Haruta, T. Kobayashi, H. Sano, N. Yamada, Chem. Lett. 2 (1987) 405.
[13] M. Haruta, S. Tsubota, T. Kobayashi, H. Kageyama, M.J. Genet, B. Delmon, J. Catal. 144 (1993) 175.
[14] S.D. Gardner, G.B. Hoflund, M.R. Davidson, H.A. Laitinen, D.R. Schryer, B.T. Upchurch, Langmuir 7 (1991) 2140.
[15] M. Daté, M. Haruta, J. Catal. 201 (2001) 221.
[16] M. Daté, M. Okumura, S. Tsubota, M. Haruta, Angew. Chem. Int. Ed. 43 (2004) 2129.
[17] M. Kang, M.W. Song, C.H. Lee, Appl. Catal. A: Gen. 251 (2003) 143.
[18] C. Tang, C. Kuo, M. Kuo, C. Wang, S. Chien, Appl. Catal. A: Gen. 309 (2006) 37.
[19] Y.Y. Yao, J. Catal. 33 (1974) 108.
[20] D. Perti, R.L. Kabel, AlChE J. 31 (1985) 1420.
[21] X. Xie, Y. Li, Z. Liu, M. Haruta, W. Shen, Nature 458 (2009) 746.
[22] M. Krämer, T. Schmidt, K. Stöwe, W.F. Maier, Appl. Catal. A: Gen. 302 (2006) 257.
[23] D.R. Merrill, C.C. Scalione, J. Am. Chem. Soc. 43 (1921) 1982.
[24] C. Yoon, D.L. Cocke, J. Catal. 113 (1988) 267.
[25] M.A. Brittan, H. Bliss, C.A. Walker, AlChE. J. 16 (1970) 305.
[26] S.B. Kanungo, J. Catal. 58 (1979) 419.
[27] G.J. Hutchings, A.A. Mirzaei, R.W. Joyner, M.R.H. Siddiqui, S.H. Taylor, Catal. Lett. 42 (1996) 21.
[28] S. Veprek, D.L. Cocke, S. Kehl, H.R. Oswald, J. Catal. 100 (1986) 250.
[29] G.J. Hutchings, A.A. Mirzaei, R.W. Joyner, M.R.H. Siddiqui, S.H. Taylor, Appl. Catal. A: Gen. 166 (1998) 143.
[30] Z.-R. Tang, C.D. Jones, J.K.W. Aldridge, T.E. Davies, J.K. Bartley, A.F. Carley, S.H. Taylor, M. Allix, C. Dickinson, M.J. Rosseinsky, J.B. Claridge, Z. Xu, M.J. Crudace, G.J. Hutchings, Chem. Catal. Chem. 1 (2009) 247.
[31] A.S. Kireev, V.M. Mukhin, S.G. Kireev, V.N. Klushin, S.N. Tkachenko, Russ. J. Appl. Chem. 82 (2009) 169.
[32] N. Tugrul, E.M. Derun, M. Piskin, Waste Manage. Res. 24 (2006) 446.
[33] C.D. Wagner, W.M. Riggs, L.E. Davis, J.F. Moulder, G.E. Mullenberg, Handbook of X-ray Photoelectron Spectroscopy, Perkin-Elmer Corp., Eden Prairie, MN, USA, 1979.
[34] H.W. Nesbitt, D. Banerjee, Am. Mineral. 83 (1998) 305.
[35] D. Glover, B. Schumm, A. Kozawa (Eds.), Handbook of Manganese Dioxide Battery Grade, International Battery Materials Association, Cleveland, OH, 1989, p. 314.
[36] V.D. Makwana, L.J. Garces, J. Liu, J. Cai, Y. Son, S.L. Suib, Catal. Today 85 (2003) 225.
[37] A.A. Mirzaei, H.R. Shaterian, M. Kaykhaii, Appl. Surf. Sci. 239 (2005) 246.
[38] D. Dollimore, K.H. Tonge, J. Chem. Soc. A (1970) 1728.
[39] R.K. Herz, A. Badlani, D.R. Schryer, B.T. Upchurch, J. Catal. 141 (1993) 219.
[40] R.M. Ziff, E. Gulari, Y. Barshad, Phys. Rev. Lett. 56 (1986) 2553.